Biaxial fatigue behavior of a powder metallurgical TRIP steel

S. Ackermann, T. Lippmann, D. Kulawinski, S. Henkel, H. Biermann
Institute of Materials Engineering, Technische Universität Bergakademie Freiberg,
Gustav-Zeuner-Str. 5, 09599 Freiberg, Germany
Stephanie.Ackermann@iwt.tu-freiberg.de

ABSTRACT. Multiaxial fatigue behavior is an important topic in critical structural components. In the present study the biaxial-planar fatigue behavior of a powder metallurgical TRIP steel (Transformation Induced Plasticity) was studied by taking into account martensitic phase transformation and crack growth behavior.

Biaxial cyclic deformation tests were carried out on a servo hydraulic biaxial tension-compression test rig using cruciform specimens. Different states of strain were studied by varying the strain ratio between the axial strain amplitudes in the range of -1 (shear loading) to 1 (equibiaxial loading). The investigated loading conditions were proportional due to fixed directions of principal strains.

The studied TRIP steel exhibits martensitic phase transformation from γ-austenite via ε-martensite into α'-martensite which causes pronounced cyclic hardening. The α'-martensite formation increased with increasing plastic strain amplitude. Shear loading promoted martensite formation and caused the highest α'-martensite volume fractions at fatigue failure in comparison to uniaxial and other biaxial states of strain.

Moreover, the fatigue lives of shear tests were higher than those of uniaxial and other biaxial tests. The von Mises equivalent strain hypothesis was found to be appropriate for uniaxial and biaxial fatigue, but too conservative for shear fatigue, according to literature for torsional fatigue. The COD strain amplitude which is based on crack opening displacement gave a better correlation of the investigated fatigue lives, especially those for shear loading. Different types of major cracks were observed on the sample surfaces after biaxial cyclic deformation by using electron monitoring in an electron beam universal system and scanning electron microscopy (SEM). Specimens with strain ratios of 1, 0.5, -0.1 and -0.5 showed mode I major cracks (perpendicular to the axis of maximum principal strain). Major cracks after shear fatigue had partially mode II orientation (tilted 45° to the loading axes) and afterwards bifurcated into two pairs of mode I cracks. Another shear test revealed a major crack of mode I orientation (parallel to the loading axes). These results are in good agreement to the literature.

Micro cracks after shear fatigue were longer than those after biaxial fatigue with strain ratios of 1 and 0.5. Major and minor cracks after equibiaxial and shear loading showed crack branching and crack coalescence.

The results on fatigue crack behavior support the assumption that the period of stage I (mode II) crack propagation is much longer under shear loading than under other biaxial conditions due to absence of tensile stress normal to the planes of maximum shear strain under shear loading.

KEYWORDS. Biaxial fatigue; Cruciform specimen; TRIP steel; Martensitic phase transformation; Surface cracks.

INTRODUCTION

The influence of different states of strain on the fatigue and crack propagation behavior has been of interest since about 40 years [1, 2]. Under low cycle fatigue conditions, the fatigue lifetime may be divided into two phases: crack initiation and crack propagation of stage I and stage II. It is known from previous work (for example [2]) that stage I cracks grow on maximum shear planes which correspond to crack mode II and stage II cracks propagate on planes of

maximum principal strain which correspond to crack mode I. Parsons and Pascoe [2] published observations of surface cracks in cruciform specimens after different biaxial low cycle fatigue loading conditions. Mostly stage I cracks were found under plane strain and shear tests before fatigue failure. But in the later fatigue lifetime regime cracks also bifurcated at each crack tips from stage I cracks to pairs of two stage II cracks in shear tests of steel AISI 304. Itoh et al. [3] investigated the fatigue behavior of steel AISI 304 at 650 °C and found stage I cracks only in shear tests, whereas other strain ratios showed stage II cracks after fatigue failure. Brown and Miller [1] proposed two types of cracks which are characterized by different crack growth directions of stage I and II cracks in dependence on the load ratio $\lambda = \Delta\sigma_2/\Delta\sigma_1$ between the principal stresses σ_1 and σ_2. Crack type A occurred under $\lambda = -1$ loading which corresponds to pure shear loading and propagated along the surface. Cracks of type B formed under equibiaxial $\lambda = 1$ loading and grew through the specimen thickness which is critical for plane stress states.

Various models have been published to assess fatigue failure in complex stress-strain conditions besides the widely used von Mises equivalent strain amplitude. For example, the Γ-plane theory of Brown and Miller [1] considers maximum shear strain and tensile strain on maximum shear plane, and the COD strain of Sakane et al. [3] is based on crack opening displacement (COD).

Biaxial fatigue has been studied by biaxial-planar tests using cruciform specimens. Principal stress and strain directions are fixed in biaxial-planar tests due to fixed perpendicular loading axes, even under biaxial loading with a phase shift φ between the controlled axial strains. Thus, no rotation of stress and strain directions occurs, in contrast to non-proportional axial-torsional tests on thin-walled tubular specimens [4]. Using cruciform specimens different states of strain can be achieved by varying phase shift φ between 0° and 180° as well as strain ratio $\Phi = \Delta\varepsilon_2/\Delta\varepsilon_1$ between -1 and 1, where ε_1 and ε_2 are principal strains [3, 5]. Loading conditions with $\Phi = -1$ and 1 correspond to pure shear and equibiaxial loading, respectively, whereas $\Phi = -0.5$ corresponds to uniaxial loading since Poisson's ratio tends to 0.5 under plastic straining.

It is known from literature that shear loading yields the highest fatigue lives compared to other biaxial loading conditions [3–9]. Itoh et al. [3] investigated strain ratios Φ of -1, -0.5, 0, 0.5, and 1 for austenitic steel AISI 304 at 650 °C. The fatigue lives ranged between those of equibiaxial ($\Phi = 1$) and shear ($\Phi = -1$) loading.

In the present study the biaxial fatigue behavior of a metastable austenitic steel is investigated for strain ratios Φ in the range of -1 to 1 at room temperature. The material was produced from powder by hot-pressing technique and is compared to a previously studied cast variant. The steel shows martensitic phase transformation from austenite via ε-martensite into α'-martensite during cyclic deformation, e.g. [10], causing cyclic hardening, see e.g. [11–13]. The aim of the present study is to clarify the influence of different states of strain on cyclic deformation behavior, crack propagation, and fatigue failure. Therefore, surface cracks were investigated by using electron monitoring with an electron beam universal system and scanning electron microscopy (SEM).

MATERIAL AND EXPERIMENTAL DETAILS

The investigated material was a metastable austenitic TRIP steel (TRansformation Induced Plasticity) with 15.3–16.3 %Cr, 5.4–7.2 %Mn, 5.8–6.5 %Ni, 0.04–0.07 %C and 0.05–0.08 %N (wt.%). The material was processed as sintered steel powder (called PM 16-7-6 in the following). Sintered discs were produced by using hot-pressing technique at 1250 °C with 30 MPa for 30 minutes. Thus, a fine grained, mainly austenitic microstructure with δ-ferrite volume fraction less than 2 % and an average grain size of 20 μm was achieved, see Fig. 1a. An austenitic TRIP cast steel 16-6-6 (%Cr-%Mn-%Ni) with similar chemical composition and a grain size up to 1.5 mm was used as reference material.

Sintered discs (diameter 140 mm) were welded into hot-rolled plates of austenitic steel AISI 304 by electron beam welding. The welds had a good connection to both materials without defects and cracks. The position of the weld was put on a position where it is uncritical for the fatigue tests, see Fig. 1b.

Fig. 1b shows the cruciform specimen geometry which is in accordance to [5, 14]. The specimen center is planar (diameter 15 mm) and of reduced thickness (1.5 mm). The cyclic tests were carried out on a servo hydraulic biaxial-planar tension-compression machine (Instron 8800) with four actuators of 250 kN capacity. The α'-martensite volume fraction was measured by using a ferrite sensor (Fischer-scope MMS PC) due to ferromagnetic behavior of α'-martensite. The sensor was attached to the polished sample surface for *in situ* measuring within a volume of about 3.14 mm² x 1.5 mm. A biaxial orthogonal extensometer with four ceramic arms and a gauge length of 13 mm was used to measure axial strains ε_A and ε_B in the specimen center on the sample surface. In biaxial-planar tests axial strains ε_A and ε_B correspond to principal strains in terms of the assumption $\varepsilon_1 > \varepsilon_2$.

Cyclic deformation tests were carried out under total strain control of axial strains ε_A and ε_B at strain rates of about $0.004 \, s^{-1}$. Different states of strain were investigated by using strain ratios $\Phi = \Delta\varepsilon_B/\Delta\varepsilon_A$ of 1 (equibiaxial loading), 0.5, -0.1, -0.5 and -1 (pure shear loading). Fig. 1c shows the triangular signals of axial strains ε_A and ε_B of in-phase tests. Both axial strain functions had equal frequency. Axial strain amplitudes for different strain ratios were determined to achieve comparable von Mises equivalent strain amplitudes $\Delta\varepsilon_{vM}/2$ which were calculated according to [15]. Biaxial in-phase tests were performed at $\Delta\varepsilon_{vM}/2$ in the range of $0.3 - 0.6 \cdot 10^{-2}$. Biaxial reference tests on a cast TRIP steel 16-6-6 were performed under in-phase loading ($\Phi = 1, -1$) and out-of-phase loading. Out-of-phase loading was set by a phase shift φ between the strain functions of the two axes A and B. Thus, strain ratio Φ changes continuously between 1 and -1 within one cycle. However, phase shifted loading by means of a cruciform specimen causes no rotating principal stress and strain directions due to fixed perpendicular loading axes, in contrast to non-proportional axial-torsional tests [4]. Fig. 1d shows axial strain courses for phase shifts φ of 45°, 90° and 135° as examples.

Uniaxial reference tests were carried out on a conventional 250 kN servo hydraulic testing system (MTS).

In the present study a von Mises type force amplitude is used to characterize the cyclic deformation behavior because the cross sectional area in cruciform specimens is unknown and numerical simulation like in [3] was not available. The von Mises type force was calculated according to [9] by using the axial forces F_A and F_B at maximum principal strain in axis A, see Eq. (1). It is assumed that yielding and hardening of the material take place in a defined cross sectional area and maximum stresses and strains occur in the specimen center (Ø 15 mm) with homogenous distributions.

$$F_{vM} = \sqrt{\left(F_A\right)^2 + \left(F_B\right)^2 - F_A F_B} \tag{1}$$
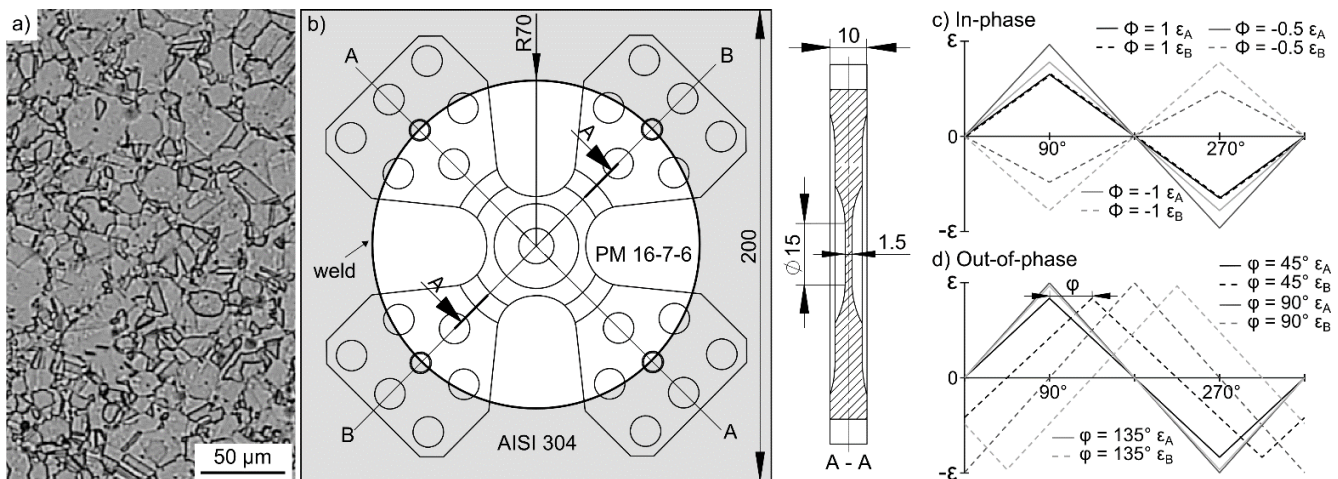
Figure 1: a) Initial austenitic microstructure of the investigated TRIP steel PM 16-7-6. b) Cruciform specimen and position of the weld in case of PM 16-7-6. Schematic courses of control signals of axial strains ε_A and ε_B for different c) strain ratios Φ (in-phase tests) and d) phase shifts φ (out-of-phase tests) at a von Mises equivalent strain amplitude $\Delta\varepsilon_{vM}/2 = 0.4 \cdot 10^{-2}$.

RESULTS AND DISCUSSION

Cyclic deformation behavior and martensitic transformation

The cyclic deformation behavior of the investigated steel was studied by means of von Mises type force amplitude $\Delta F_{vM}/2$. Fig. 2a presents the cyclic deformation curves for strain ratios Φ of 1 (equibiaxial), 0.5, -0.1, -0.5 and -1 (shear) at a von Mises equivalent strain amplitude $\Delta\varepsilon_{vM}/2$ of $0.4 \cdot 10^{-2}$. Three stages are visible independent of the state of strain: i) primary hardening, ii) softening and iii) secondary hardening. This behavior is known from uniaxial reference tests and literature on TRIP steels [11 – 13]. The course of $\Phi = 0.5$ had nearly the same evolution as the course of $\Phi = 1$. The level of the curves of negative strain ratios declined with decreasing strain ratio from -0.1 to -1. Furthermore, the onset and the magnitude of secondary hardening were the latest and the smallest for $\Phi = -0.1$ and -0.5 loading,

respectively. The earliest onset and the highest secondary hardening was found for the $\Phi = -1$ case. An analogous trend was observed for the fatigue lifetimes: the smallest was found for $\Phi = -0.1$ and -0.5 and the highest for $\Phi = -1$.

The authors conclude that shear loading ($\Phi = -1$) supported yielding and resulted in lower maximum axial forces, as reported also for cast TRIP steel [9]. Moreover, shear loading showed the most pronounced secondary hardening due to the earliest onset of hardening and the highest fatigue lifetime. The von Mises type force amplitude correlated the cyclic deformation curves of positive strain ratios well, but was not appropriate for negative strain ratios, in particular shear loading. The cross sectional areas in tests with different strain ratios were not equivalent as assumed for the von Mises type force amplitude. Further experiments revealed that the onset of secondary hardening was shifted to lower number of cycles and the magnitude of secondary hardening increased with increasing von Mises strain amplitude $\Delta\varepsilon_{vM}/2$ in the range of 0.3 to $0.6\cdot10^{-2}$ due to higher plastic deformation. The cyclic hardening depends on the plastic strain amplitude.

The investigated steel PM 16-7-6 showed a martensitic phase transformation during cyclic deformation. Fig. 2b presents the α'-martensite volume fraction vs. number of cycles of an uniaxial reference test and the biaxial tests at a von Mises equivalent strain amplitude $\Delta\varepsilon_{vM}/2 = 0.4\cdot10^{-2}$. A pronounced increase in α'-martensite content was observed after an incubation period and correlated with the onset of secondary hardening. The latest onset of martensite formation was found for $\Phi = 0.5$ and $\Phi = 1$. The other states of strain ($\Phi = -0.1, -0.5, -1$, uniaxial) showed similar courses. The α'-martensite volume fraction at fatigue failure was the lowest for $\Phi = 0.5$ (about 5 vol.%) and the highest for $\Phi = -1$ as well as uniaxial loading (up to 45 vol.%). The authors conclude that α'-martensite formation depended on plastic strain amplitude and caused the secondary hardening which is in good agreement to observations reported for uniaxial tests in literature [11–13]. Moreover, shear and uniaxial loading promoted α'-martensite formation, whereas the α'-martensite content was significantly lower in all other investigated biaxial states of strain.
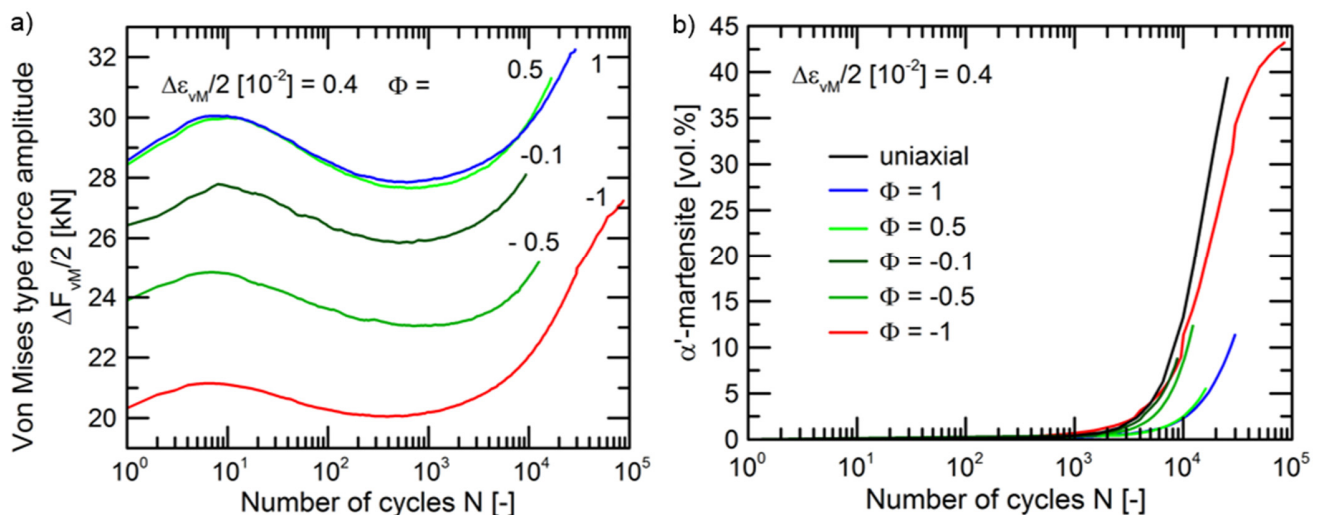
Figure 2: a) Cyclic deformation curves and b) α'-martensite evolutions of TRIP steel PM 16-7-6 at von Mises equivalent strain amplitude $\Delta\varepsilon_{vM}/2 = 0.4\cdot10^{-2}$ for different strain ratios Φ.

Fig. 3 presents the α'-martensite volume fraction at fatigue failure of the steel PM 16-7-6 plotted vs. the von Mises equivalent strain amplitudes $\Delta\varepsilon_{vM}/2$ and vs. the number of cycles to failure N_f of uniaxial and biaxial tests. A small amount of martensite (< 8 vol.%) was observed at a von Mises equivalent strain amplitude $\Delta\varepsilon_{vM}/2$ of about $0.3\cdot10^{-2}$, see Fig. 3a. Higher strain amplitudes resulted in higher α'-martensite contents due to higher plastic deformation. The highest α'-martensite content up to 85 vol.% was observed at $\Delta\varepsilon_{vM}/2 = 0.6\cdot10^{-2}$ for shear loading. Under uniaxial loading similar martensite volume fractions were observed as under shear loading. The martensite contents were considerably lower than those under biaxial shear loading at strain ratios $\Phi > -1$. An analogous trend was observed for the cyclic hardening.

Fig. 3b shows an increase in fatigue lifetime with decreasing α'-martensite content (and decreasing $\Delta\varepsilon_{vM}/2$) for the investigated uniaxial and biaxial tests ($\Phi = 1$ and -1) which is in good agreement to uniaxial findings reported elsewhere [13]. Regarding the loading conditions the following trend was observed: The lowest α'-martensite volume fractions were observed for $\Phi = -0.5, -0.1, 0.5$ followed by $\Phi = 1$ and uniaxial loading. The highest α'-martensite contents developed in

Φ = -1 tests. Shear fatigue caused both the highest α'-martensite contents and the highest fatigue lives, whereas loading with Φ = -0.5, -0.1, and 0.5 resulted in the lowest α'-martensite contents as well as the lowest fatigue lives.
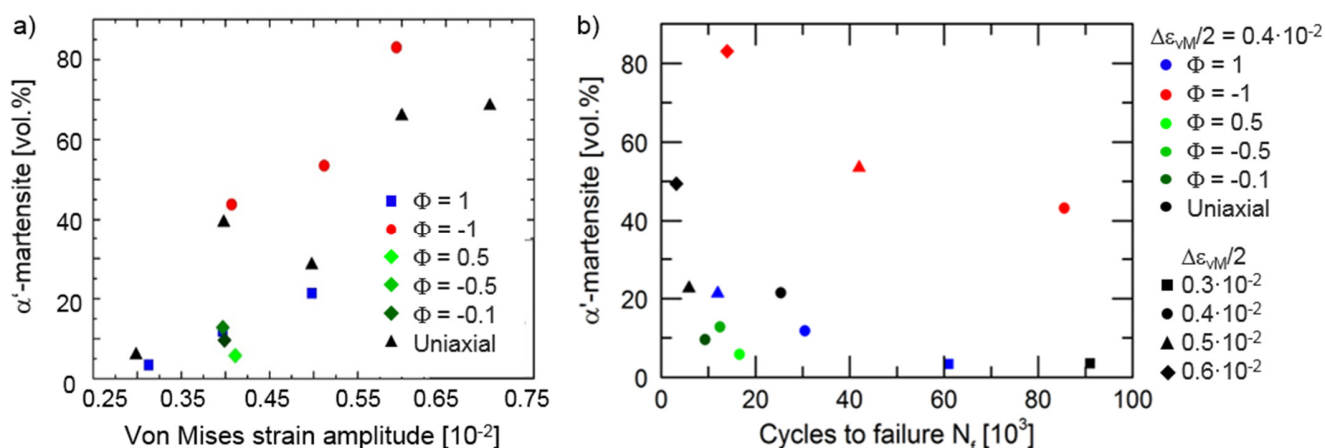
Figure 3: Correlation of α'-martensite content of the steel PM 16-7-6 at fatigue failure vs. a) von Mises equivalent strain amplitude $\Delta\varepsilon_{vM}/2$ and b) number of cycles to failure N_f for uniaxial and biaxial tests at different strain ratios Φ.

Microstructure
Fig. 4a shows a typical microstructure of PM 16-7-6 steel after cyclic deformation obtained by scanning electron microscopy in back-scatted electron contrast. The α'-martensite formed as lenses within deformation bands of a certain width, preferentially at intersection points of two deformation bands which is in good agreement to the literature e.g. [10, 16]. Thin deformation bands contained no α'-martensite nuclei which is in accordance to [10]. Transmission electron microscopy and electron channeling contrast imaging revealed that deformation bands consist of a high density of stacking faults which result in a hexagonal crystal structure, called ε-martensite, see e.g. [10].
Electron backscatter diffraction (EBSD) measurements were done after cyclic deformation on vibrational polished specimen surfaces. Phase maps showing austenite (fcc), ε-martensite (hexagonal) and α'-martensite (bcc) are presented in Fig. 4b to 4d for Φ = 1, Φ = -1, and Φ = 0.5 at a von Mises equivalent strain amplitude $\Delta\varepsilon_{vM}/2 = 0.4 \cdot 10^{-2}$. The bcc phase was always found inside the hexagonal regions. Thus, phase transformation from austenite into α'-martensite occurs via ε-martensite as an intermediate structure. Comparing different loading conditions, higher volume fractions of α'-martensite and ε-martensite of about 20 % were observed after shear loading. In contrast, only small α'-martensite and ε-martensite regions were found after equibiaxial cycling. The most intensive ε-martensite formation was obtained in the specimen after biaxial fatigue loading with Φ = 0.5, although the α'-martensite regions were small. Moreover, martensitic transformation around cracks was observed for all investigated conditions (not shown here) due to intensive plastic deformation in the plastic zone around the crack tip. This is under consideration for further detailed investigations. The EBSD results showing local phase distributions within an area of 0.53 mm x 0.4 mm were consistent with the martensite volume fractions obtained by the ferrite sensor (compare Fig. 3a).

Fatigue Life
Fig. 5a shows the fatigue lives under uniaxial and biaxial loading of the powder metallurgical steel (PM 16-7-6) in comparison to data of cast steel 16-6-6 [9] by using von Mises equivalent strain hypothesis. The lowest fatigue lives of all investigated loading conditions of PM 16-7-6 were observed for biaxial loading with strain ratios Φ of 0.5, -0.1 and -0.5. However, they ranged in the scatter band of factor two of the uniaxial fatigue lives as well as the equibiaxial (Φ = 1) fatigue lives. Thus, the uniaxial Basquin–Manson-Coffin (BMC) relationship is conservative for biaxial loading of the investigated TRIP steel. In contrast to the present study, Itoh et al. [3] observed fatigue lives for Φ = 0.5, 0 and -0.5 between those of equibiaxial (Φ = 1) and shear (Φ = -1) tests on steel AISI 304 at 650 °C.
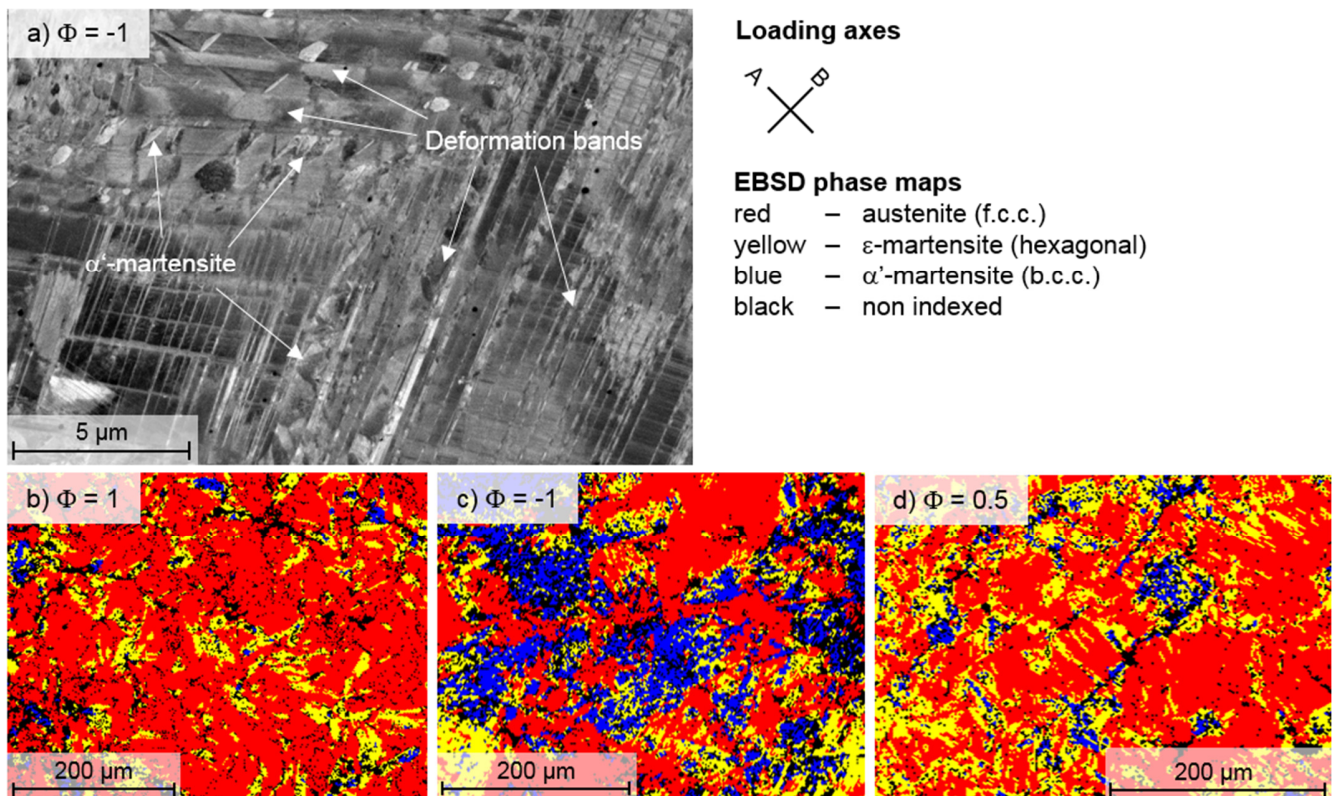
Figure 4: TRIP steel PM 16-7-6: a) SEM micrograph (backscattered electron contrast) showing deformation bands and α'-martensite after cycling with Φ = -1 (shear loading) at $\Delta\varepsilon_{vM}/2$ = 0.4·10⁻². EBSD phase maps after cycling with b) Φ = 1 (equibiaxial loading), c) Φ = -1 and d) Φ = 0.5 at $\Delta\varepsilon_{vM}/2$ = 0.4·10⁻²:

The same behavior as for Φ of 0.5, -0.1 and -0.5 was observed for out-of-phase tests with phase shifts φ = 22.5°, 45°, 90° and 135° on TRIP cast steel 16-6-6. The fatigue lives ranged within a factor two scatter band of the equibiaxial tests [9], see Fig. 5a. A phase shift caused no reduction of the fatigue life of the studied TRIP steel which is contrary to results for AISI 316FR at 550 °C [6] and for α-brass at room temperature [7].

The number of cycles to failure of shear tests (Φ = -1) were up to 7 times and 8.5 times higher than those of uniaxial tests and equibiaxial tests (Φ = 1), respectively. The differences in the fatigue lives decreased with increasing von Mises equivalent strain amplitude due to increasing plastic deformation. Similar results were observed for the cast steel 16-6-6 under equibiaxial and shear loading as reported in [9]. The observation, that the highest fatigue lives were obtained under shear loading in comparison to uniaxial and other biaxial loading conditions, is in good agreement to the literature of biaxial-planar tests [3–8] and torsional tests [17–19]. The difference between torsional and uniaxial fatigue lives is very pronounced for austenitic steels with a low stacking fault energy [18]. Different crack growth behavior as well as crack directions on the specimen surface were reported in the literature for several straining conditions [1–3]. Therefore, investigations on surface cracks are discussed later in detail. The authors assume that the period of stage I crack propagation in the plane of maximum shear strain (mode II) is much longer under shear loading than under other biaxial conditions.

Comparing powder metallurgical and cast steel variants, the fatigue lives of PM 16-7-6 were higher than those of cast 16-6-6 steel: for uniaxial and Φ = 1 loading, the factor is 3–7 and for Φ = -1 loading it is about 2 (in the range $\Delta\varepsilon_{vM}/2$ of 0.6·10⁻² to 0.3·10⁻²). That means, that the factor between fatigue lives of shear and those of equibiaxial loading was lower for PM 16-7-6 than for cast 16-6-6 steel, especially with decreasing von Mises equivalent strain amplitude.

Microstructural investigations revealed different grain sizes and types of defects in the materials due to production processes. The grains of the cast steel variant were up to 75 times greater than those of the PM steel variant. Shrinkage cavities in the cast steel [9] had larger dimensions than impurities in the powder metallurgical steel. Furthermore, the yield stress of the PM steel (about 266 MPa) was about 1.18 times higher than that of the cast steel (about 225 MPa). As a conclusion, the powder metallurgical TRIP steel variant (PM 16-7-6) is more tolerant with respect to fatigue failure than the cast TRIP steel variant.

Fig. 5b shows the fatigue lifetimes vs. COD strain amplitude of PM 16-7-6 for uniaxial and biaxial loading cases ($-1 \leq \Phi \leq 1$). The COD strain gave a good correlation of uniaxial and all investigated biaxial fatigue lives including those for shear within a scatter band of factor two. The COD criterion proposed by Sakane et al. [3] is based on crack opening displacement and considers the smaller crack opening in shear loading case.
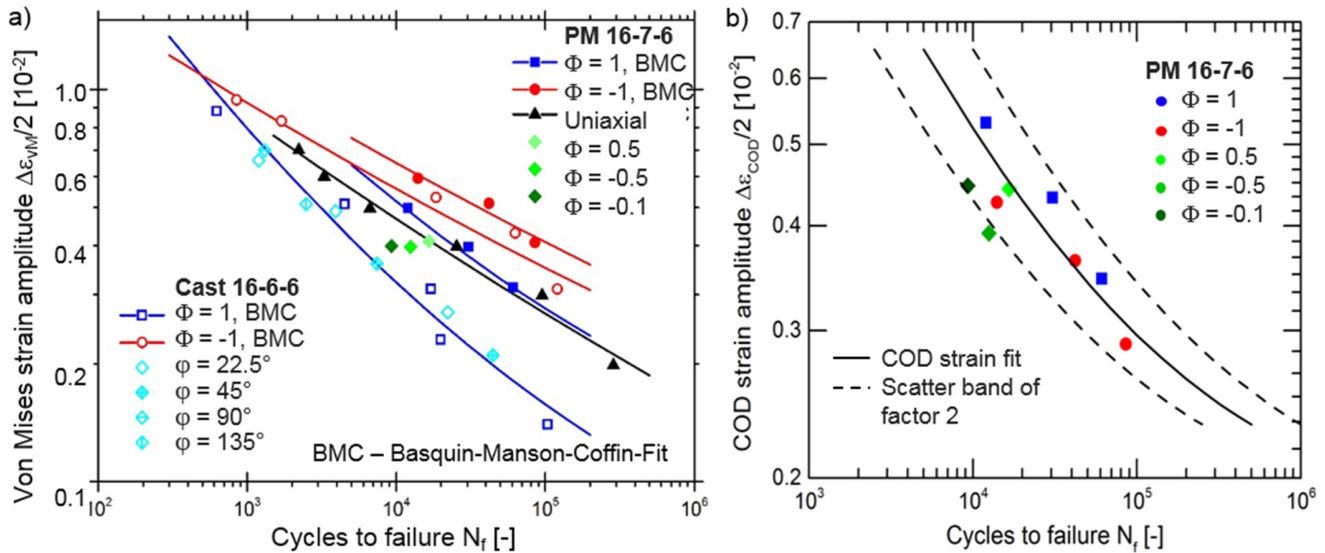
Figure 5: Fatigue lives N_f of PM steel 16-7-6 and cast steel 16-6-6 [9] under uniaxial and biaxial cyclic straining (strain ratio Φ, phase shift φ) vs. a) von Mises equivalent strain amplitude $\Delta\varepsilon_{vM}/2$ and b) COD strain amplitude $\Delta\varepsilon_{COD}/2$ according to [3].

Surface cracks

Crack directions of the major cracks which caused fatigue failure were studied on the specimen surface by using electron monitoring in an electron beam universal system since specimen dimensions were too large for SEM. Fig. 6 shows the major cracks in the specimen centers after cycling with $\Phi = 1$, -1 and 0.5. The major crack was often observed at the transition radius of the specimens (indicated by circles in Fig. 6) which is caused by slight notch effects, as also reported in [5]. The major cracks were oriented at an angle of 45° to the loading axes A and B under equibiaxial loading ($\Phi = 1$, Fig. 6a) and perpendicular to the axis of maximum principal strain for strain ratios Φ of 0.5, -0.1, -0.5 and -1 at $\Delta\varepsilon_{vM}/2 = 0.4 \cdot 10^{-2}$ (Fig. 6b). These surface cracks propagated in planes of maximum principal strain which correspond to stage I (mode II), see [1, 3]. This result is in agreement with the assumption of Brown and Miller [1] who proposed a crack type for equibiaxial loading which grows through the thickness and results in lower fatigue lifetimes. On the other hand, shear straining at $\Delta\varepsilon_{vM}/2 = 0.5 \cdot 10^{-2}$ (Fig. 6d) and $0.6 \cdot 10^{-2}$ revealed major cracks in the specimen center which propagated at first under an angle of 45° to the loading axes A and B. This direction indicated crack propagation in the plane of maximum shear strain which correspond to stage I crack growth (mode II). Subsequently, the major crack bifurcated into two pairs of cracks parallel to the loading axes A and B. Thus, a transition from stage I to stage II occurred. These findings are in good agreement to the results of Parsons and Pascoe [2] who found that stage I crack growth is dominant in the shear experiments prior to fatigue failure. Moreover, they also observed crack bifurcation at each crack tip with transition from stage I to stage II crack growth fairly late in fatigue life of AISI 304 stainless steel. Itoh et al. [3] found also cracks propagating in the maximum shear strain directions (mode II or stage I) only in shear tests, whereas other investigated strain ratios showed stage II cracks (mode I). The results of the present study support the assumption presented in literature [2] that the period of stage I (mode II) crack propagation is much longer under shear loading than under other biaxial conditions. For shear loading there is no tensile stress normal to the planes of maximum shear strain unless the crack path is deflected by material inhomogeneities or crack linking.

Scanning electron microscopy was used for further investigations of the major cracks as well as cracks between 0.05 and 0.7 mm in length on the specimen surface. Fig. 7 shows major cracks with length greater than 1 mm and minor cracks smaller than 0.1 mm in length after fatigue failure under shear ($\Phi = -1$) and equibiaxial ($\Phi = 1$) loading, respectively. The major crack after shear loading (Fig. 7a) was nearly straight over wide distances and had smooth crack surfaces in contrast to the major crack after equibiaxial loading (Fig. 7b) which showed a distinct zig-zag path with several kinks. Crack branching was

observed for the major cracks (Fig. 7a and 7b) as well as for minor cracks (Fig. 7c and 7d) under both straining conditions. The investigated minor cracks had crack lengths of maximum 0.2 mm after equibiaxial cycling and maximum 0.7 mm after shear cycling. They extended mostly over several grains and crack linkage was observed as well. Minor cracks after equibiaxial loading showed different directions (Fig. 7d), whereas most investigated cracks after shear loading were oriented parallel to the loading axes A and B (Fig. 7c). These cases correspond to mode I crack directions. However, a few cracks with 45° orientation to the loading axes which corresponds to mode II were observed in the shear specimen as well (Fig. 7c). The mode II orientation was found for crack lengths between 0.05 and 0.13 mm, thereafter these cracks branched into two mode I cracks. Locally, cracks propagated along deformation bands. Crack initiation was mostly found on impurities, but also in the matrix along deformation bands (e.g. Fig. 7c).
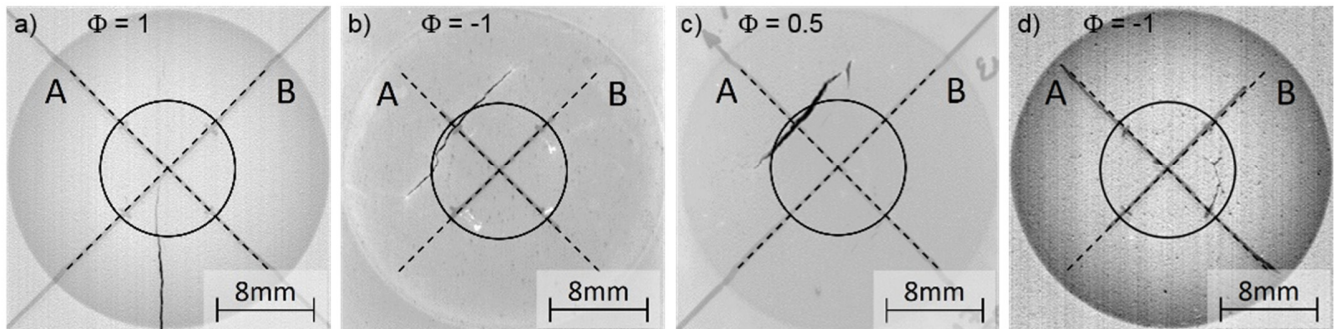
Figure 6: Surface cracks after biaxial fatigue of steel PM 16-7-6 with strain ratios of a) $\Phi = 1$ (equibiaxial loading), b) $\Phi = -1$ (shear loading) and c) $\Phi = 0.5$ at $\Delta\varepsilon_{vM}/2 = 0.4\cdot10^{-2}$ (a, b, c) as well as d) $\Phi = -1$ at $\Delta\varepsilon_{vM}/2 = 0.5\cdot10^{-2}$, obtained by electron beam monitoring of the gauge area indicated by circles, loading axes A and B marked.
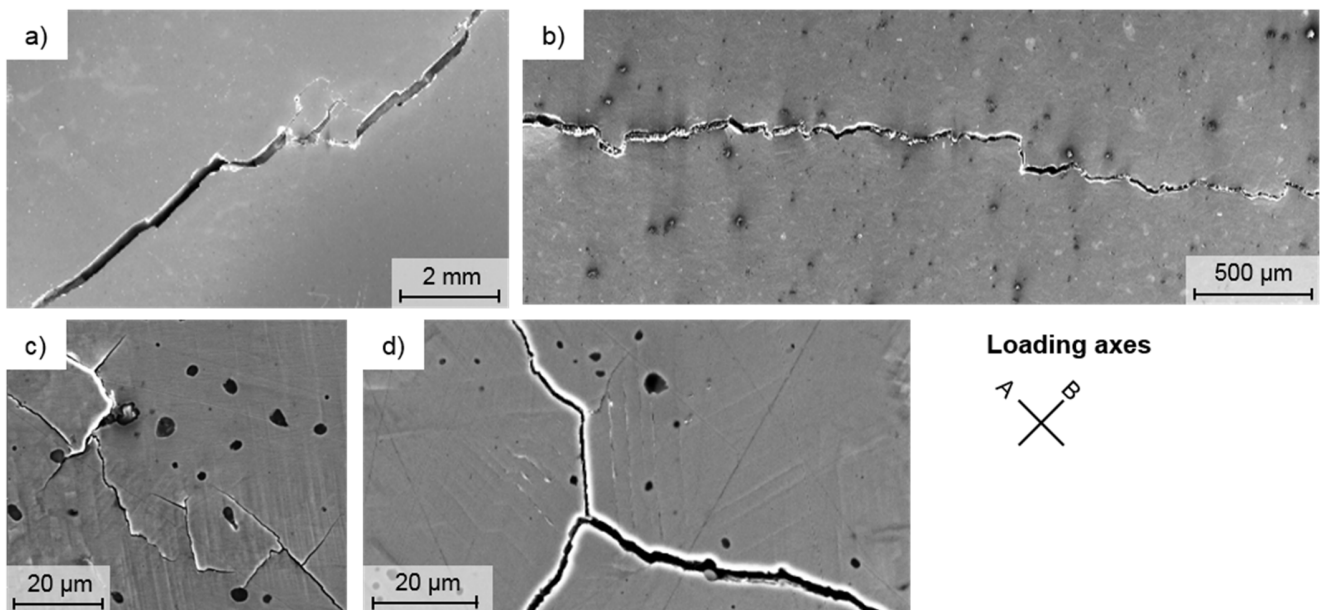
Figure 7: Micrographs of surface cracks after biaxial cycling with $\Phi = -1$ (a, c) and $\Phi = 1$ (b, d) at $\Delta\varepsilon_{vM}/2 = 0.4\cdot10^{-2}$ of TRIP steel PM 16-7-6. Major cracks (a, b) and cracks smaller than 0.1 mm (c, d) show crack branching.

SUMMARY

The cyclic deformation and fatigue behavior of a metastable austenitic TRIP steel was investigated under uniaxial and different biaxial-planar loading conditions and discussed by using observations of surface cracks.

Shear fatigue caused both the highest number of cycles to failure and the highest α'-martensite volume fractions, whereas loading with $\Phi = -0.5$, -0.1 and 0.5 resulted in the lowest fatigue lives as well as the lowest α'-martensite contents.

By using EBSD measurements large areas of α'-martensite and ε-martensite were observed after shear loading and only small α'-martensite and ε-martensite regions were found after equibiaxial cycling. The specimen loaded under Φ = 0.5 fatigue showed the most intensive ε-martensite formation, although the α'-martensite regions were small.

The fatigue lives of Φ of 0.5, -0.1 and -0.5 tests were the lowest of all investigated loading conditions by using von Mises equivalent strain hypothesis, but ranged in the scatter band of the fatigue lives of uniaxial and equibiaxial (Φ = 1) tests. Thus, the uniaxial Basquin–Manson-Coffin relationship is conservative for biaxial loading of the investigated TRIP steel. The highest fatigue lives were observed under shear loading in comparison to uniaxial and other investigated biaxial loading conditions which is in good agreement to the literature of biaxial-planar and torsional tests. The COD strain proposed by Sakane et al. [3] based on crack opening displacement gave a good correlation of all investigated fatigue lives including those for shear.

The fatigue lives for the TRIP steel PM 16-7-6 were higher than those of the cast steel 16-6-6 unser the same loading conditions. This effect was smaller under shear loading than under equibiaxial loading. Furthermore, the factor between fatigue lives of shear and those of equibiaxial loading was lower for PM 16-7-6 than for cast 16-6-6. Different defects in the materials due to production processes were observed by scanning electron microscopy.

Observations of surface cracks after fatigue failure revealed that most of the major and minor cracks had mode I direction which corresponds to stage II crack propagation in the plane of maximum principal strain. However, the major cracks of two shear tests showed mode II (stage I) crack propagation in the plane of maximum shear strain. Subsequently, the stage I major cracks bifurcated into two pairs of mode I cracks (stage II). These observations are in good agreement to the literature. The same behavior was observed for a few minor cracks with length between 0.05 and 0.13 mm. Furthermore, the investigated minor cracks after shear loading had much larger length than minor cracks after equibiaxial loading. The results support the assumption that the period of stage I (mode II) crack propagation is much longer under shear loading than under other biaxial conditions due to absence of crack opening stresses.

REFERENCES

[1] Brown, M.W., Miller, K.J., A Theory for Fatigue Failure under Multiaxial Stress-Strain Conditions, Proc. Inst. Mech. Eng., 187 (1973) 745–55. DOI: 10.1243/PIME_PROC_1973_187_161_02.

[2] Parsons, M.W., Pascoe, K.J., Observations of surface deformation, crack initiation and crack growth in low-cycle fatigue under biaxial stress, Mater. Sci. Eng., 22 (1976) 31–50. DOI: 10.1016/0025-5416(76)90133-6.

[3] Itoh, T., Sakane, M., Ohnami, M., High temperature multiaxial low cycle fatigue of cruciform specimen, Trans. ASME, 116 (1994) 90–98. DOI: 10.1115/1.2904261.

[4] Shamsaei, N., Fatemi, A., Socie, D.F., Multiaxial fatigue evaluation using discriminating strain paths, Int. J. Fatigue, 33 (2001) 597–609.

[5] Pascoe, K.J., de Villiers, J.W.R., Low cycle fatigue of steels under biaxial straining, J. Strain Anal. Eng. Des., 2 (1967) 117–1126. DOI: 10.1243/03093247V022117.

[6] Ogata, T., Takahashi, Y., Eur. Struct. Integr. Soc., 25 (1999) 101–114. DOI: 10.1016/S1566-1369(99)80010-7.

[7] Henkel, S., Fischer, J., Balogh, L., Ungar, T., Biermann, H., Low-cycle fatigue behaviour and microstructure of copper and alpha-brass under biaxial load paths, J. Phys., 240 (2010) 012042. Doi:10.1088/1742-6596/240/1/012042.

[8] Kulawinski D., Ackermann, S., Glage, A., Henkel, S., Biermann, H., Biaxial Low Cycle Fatigue Behavior and Martensite Formation of a Metastable Austenitic Cast TRIP Steel Under Proportional Loading, Steel Res. Int., 82 (2011) 1141–1148. DOI: 10.1002/srin.201100111.

[9] Ackermann, S., Kulawinski, D., Henkel, S., Biermann, H., Biaxial in-phase and out-of-phase cyclic deformation and fatigue behavior of an austenitic TRIP steel, Int. J. Fatigue, 67 (2014) 123–133. DOI:10.1016/j.ijfatigue.2014.02.007.

[10] Weidner, A., Glage, A., Biermann, H., In-situ characterization of the microstructure evolution during cyclic deformation of novel cast TRIP steel, Proc. Eng., 2 (2010) 1961–1971. DOI: 10.1016/j.proeng.2010.03.211.

[11] Bayerlein, M., Christ, H.-J., Mughrabi, H., Plasticity-induced martensitic transformation during cyclic deformation of AISI 304L stainless steel, Mater. Sci. Eng. A, 114 (1989) L11–L16. DOI: 10.1016/0921-5093(89)90871-X.

[12] Krupp, U., West, C., Christ, H.-J., Deformation-induced martensite formation during cyclic deformation of metastable austenitic steel: Influence of temperature and carbon content, Mater. Sci. Eng. A, 481–482 (2008) 713–717. DOI: 10.1016/j.msea.2006.12.211.

[13] Glage, A., Weidner, A., Biermann, H., Cyclic Deformation Behaviour of Three Austenitic Cast CrMnNi TRIP/TWIP Steels with Various Ni Content, Steel Res. Int., 82 (2011) 1040–1047. DOI: 10.1002/srin.201100080.

[14] Scholz, A., Samir, A., Berger, C., Biaxial thermomechanical fatigue experiments with cruciform test pieces, In: Sonsino, C.M., Zenner, H., Portella, P.D. (Eds.), Proc. 7th of Int. Conf. on Biaxial and Multi-axial Fatigue & Fracture, Elsevier, Berlin, (2004) 555–560.

[15] Sonsino, C.M., Grubisic, V., Kurzzeitschwingfestigkeit von duktilen Stählen unter mehrachsiger Beanspruchung, Materialwiss. Werkst., 15 (1984) 378–386.

[16] Olson, G.B., Cohen, M., Kinetics of strain-induced martensitic nucleation, Metall. Trans. A, 6 (1975) 791–795. DOI 10.1007/BF02672301.

[17] Yokobori, T., Yamanouchi, H., Yamamoto, S., Low cycle fatigue of thin-walled hollow cylindrical specimens of mild steel in uni-axial and torsional tests at constant strain amplitude, Int. J. Fract. Mech., 1 (1965) 3–13.

[18] Doquet, V., Crack initiation mechanisms in torsional fatigue, Fatigue Fract. Eng. Mater. Struct., 20 (1997) 227–35. DOI: 10.1111/j.1460-2695.1997.tb00280.x.

[19] Nitta, A., Ogata, T., Kuwabara, K., Fracture mechanisms and life assessment under high-strain biaxial cyclic loading of type 304 stainless steel, Fatigue Fract. Eng. Mater. Struc., 12 (1989) 77–92. DOI: 10.1111/j.1460-2695.1989.tb00515.x.